RF Breakdown in High Vacuum Multimegawatt X-band Structures

Valery A. Dolgashev and Sami G. Tantawi

SLAC, Stanford, CA 94309, USA

Abstract. Increasing the power handling capabilities of rf components is an important issue for the design of rf accelerators and rf sources. RF breakdown is a phenomena that limit the high power performance. A major concern is the damage that can occur in rf components from breakdown. To better understand this damage, we have studied rf breakdown in a rectangular waveguide experimentally and theoretically. The breakdown process in a waveguide is both easier to measure and simulate than breakdown in a complex geometry such as an accelerating structure. We used a particle tracking code and a Particle-In-Cell code to model the breakdown behavior. Models developed for the waveguide were applied to the breakdown in accelerating structures. RF breakdown in traveling wave and standing wave accelerating structures was simulated. We compare the experimental data with results of the simulations for the accelerating structures.

INTRODUCTION

Accelerating gradient is one of the crucial parameters affecting design, construction and cost of next-generation linear accelerators. For a specified final energy, the gradient sets the accelerator length, and for a given accelerating structure and pulse repetition rate it determines power consumption. Accelerating gradients on the order of 100 MV/m have been reached in short (~ 20 cm) standing wave and traveling wave X-band accelerating structures [1, 2, 3]. But recent experiments have shown damage to traveling wave accelerating structures at gradients as low as 50 MV/m after 1000 hours of operation [4]. RF breakdown is a probable cause of this damage. An extensive experimental and theoretical program to determine a safe operating gradient for the Next Linear Collider (NLC) is under way in SLAC. The present work is a part of that program.

RF breakdown

We define rf breakdown as a phenomenon that abruptly and significantly changes transmission and reflection of the rf power directed to the structure under test. We distinguish breakdown from field emission and dark current. Dark currents have reproducible and monotonic (with respect to input power) behavior in spite their random space-time origin. There is evidence [4] that rf breakdown can damage the structure. RF breakdown is a complex phenomenon and its physics is yet to be understood. It includes the rf driven interaction of electrons, ions and neutral atoms, heating and melting of the metal surface *etc*. The short time scale of the breakdown (~ 5 ns–10 μs), its unpredictable starting time, and the random location of the breakdown site make it very difficult to observe its microscopic behavior. In contrast, we routinely detect and record external

macroscopic parameters such as incident rf power, power reflected from the breakdown site, and power transmitted through it. We use other parameters, such as emitted light, X-rays and harmonics of the working frequency to obtain more information about the physics of the breakdown phenomenon. Other parameters are the electron currents that exit from the beam pipe of the accelerating structure.

Simulations

We use a simplified physical model to simulate the breakdown. We assume that part of the structure surface starts emitting electron and ion currents at a predetermined time (the physics of this emission are not considered here). We adjust the emission models to resemble observed parameters (transmitted and reflected rf) of the experimental data. We have chosen a commercial Particle-In-Cell (PIC) code MAGIC [6] for these simulations. This code is used at SLAC for 2D and 3D simulation of klystrons. Such features of the code as the capability for input of realistic geometries and developed diagnostics (of particle and field parameters) make it very useful for the simulations. Unfortunately, the chosen code does not let us use small emission areas. Traces left by breakdowns on metal surfaces have a size $\sim 10 - 100 \ \mu$m and the smallest mesh size in the PIC code is ~ 1 mm. Another limitation is the maximum size of the simulated structure. We have simulated up to 8 cells (~ 10 cm) of 11.4 GHz standing wave accelerating structure in 2D and 5 cells (~ 5 cm) of traveling wave structure in 3D, while real structures have lengths up to 1.8 m. The simulations were guided by comparison with measurements of breakdown in a simple rectangular waveguide. The breakdown process in a waveguide is both easier to measure and to simulate than breakdown in the complex geometry of an accelerating structure.

BREAKDOWN IN A WAVEGUIDE

Experiment

As part of the breakdown research program we studied rf breakdown in a rectangular waveguide.

Its width was reduced to 1.33 cm (in comparison with a width of 2.29 cm for WR90) over a length of 6 cm in order to enhance the electric field by lowering the group velocity to 0.18c, and force the breakdown to occur in a this area. The height of the waveguide is 1.02 cm. We subjected the waveguide to rf power up to 120 MW with pulse widths up to 1.2 μs. We recorded incident, transmitted and reflected rf power; intensity of light emission and its spectrum; intensity of X-rays; and harmonics of the working frequency of 11.424 GHz. Harmonics were present in the klystron output as well as being generated by rf breakdown. We list some general conclusions about breakdown behavior deduced from the results of this experiment:

1. Transmitted power has a repeatable shape: it drops off to zero with an amplitude proportional to $e^{\frac{-(t-t_s)^2}{2\tau^2}}$ (Gaussian-like). Here t_s is breakdown start time. The rf pulse starts at $t = 0$. The range of the drop off time constant τ is between 10 and 200 ns. For a preprocessed waveguide τ is ~ 30 ns. Here preprocessing means

steady running at ~ 100 MW of rf power through the waveguide with a short pulse length ~ 300 ns.

2. Transmission does not recover for several microseconds after the breakdown.
3. During the Gaussian drop off the transmitted and often the reflected signals have a few oscillations.
4. Up to 90% of the incident rf energy is absorbed after $t_s + 2\tau$. Breakdowns in a preprocessed waveguide absorb (on average) less energy than otherwise.
5. RF transmission fully recovers after the main rf pulse has been off for several milliseconds.
6. Light (emitted from the breakdown site) lasts for several microseconds after the rf pulse.
7. Spectral lines of the light are mostly from neutral copper atoms (Cu I) with traces of Cu II ions and hydrogen.
8. Breakdowns tend to occur on sequences of rf pulses. Subsequent breakdowns most probably have a shorter starting time t_s than the first breakdown of a sequence.
9. Breakdowns at rf high power (~ 100MW) and short pulse length (~ 300 ns) decrease dark currents, and lower power and a longer pulse (more than 400 ns) increases dark currents. We think that the level of dark currents indicates the degree of metal surface damage.
10. Breakdown has no detectable effect on laser light (632.8 nm) passing through the waveguide .
11. In most events, the 3rd harmonic (34.272 GHz) signal from the klystron transmitted through the breakdown site is shut off by the breakdown.
12. Breakdown produces a 3rd harmonic of the klystron signal, and, probably, higher harmonics.
13. Characteristic size of the damaged spots on the surface of the waveguide is ~ 10–$100\,\mu$m.

Simulations

We performed 3D PIC simulations of the breakdown in the waveguide. The waveguide model has the same cross section as the experiment and a length of 6 cm. There is no reflection from the waveguide's ends for the TE01 mode. We simulated breakdown by creating emission spots on the broad walls of the waveguide. We applied space-charge limited emission of electrons. For that we used the built-in code feature EMISSION EXPLOSIVE. For copper ions we used a beam generated at the same area with a predetermined current density and initial velocity distribution (BEAM model in MAGIC). We changed such parameters as size and position of the emitting spots, input power, initial characteristics of the ion beam, and density of a neutral gas. We varied the size of the emitting spots from 1.6 mm$\times$1.6 mm up to 1 cm$\times$4 cm. From this numerical experiment we came to the conclusions listed below.

1. The major energy exchange between incident rf fields and particles comes from the interaction of the rf electric fields with electrons (not with ions). Electrons cross the
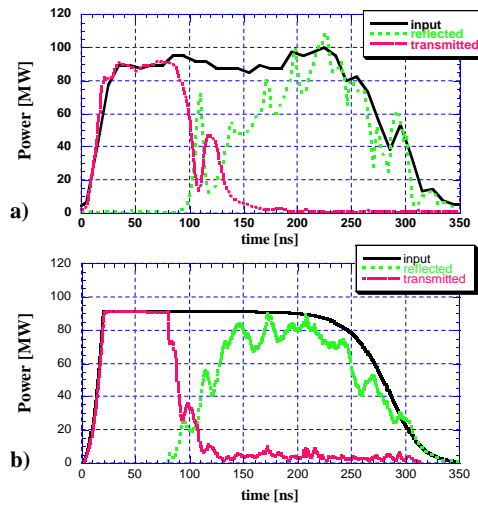
FIGURE 1. Incident, reflected and transmitted rf power for a breakdown in the waveguide. a) a measurement of a typical breakdown in the preprocessed waveguide. b) 3D PIC simulations, with an emitting spot size 4 mm×4 mm, an electron current of 7 kA, and a copper ion current of 30 A.

waveguide in a short time ($\sim$ rf period).

2. The electron current must be several kA to significantly effect the rf power transmission. If we take into account the size of the damaged area, the current density must be in the order of 10^7 A/cm^2. Space charge-limited emission of electrons without ions cannot produce and sustain such current densities.

3. Ion currents must be 10 to 100 A to disrupt transmitted power. An initial energy up to 50 eV does not change the ion dynamics. The space charge fields of the ions compensates the electron space charge fields. This compensation allows the generation of kA of electron current. The time constant of the drop off of the transmitted power τ is 10 to 20 ns and is related mostly to the process of filling the waveguide gap with copper ions.

4. Without electrons the ions do not move significantly during the rf pulse. In the presence of space-charge limited electron flow, the ion beam crosses the waveguide in about 30 ns at 80 MW of input power. The oscillating space charge field of the electrons adds a dc component to the rf electric field that accelerates the ions.

5. A significant portion (50–80%) of the emitted electrons and ions returns to the emitting spot and the surrounding area.

6. During the rf pulse, most electrons and ions are confined to a beam with a cross-section area of about 1 cm^2.

7. The transmitted and reflected power oscillates with a period 10–40 ns, determined by the ion-electron density.

8. The ion-electron current generates harmonics of the working frequency. The perturbation of the incident electric field due to these harmonics is on the order of 10%.

9. Up to 50% of the input power can be absorbed by the ion-electron beam.

10. Up to 75% of the input power was absorbed by the ion-electron beam after we added some effects associated with the interaction of electrons with neutral copper atoms.

A comparison between a signal from an typical actual breakdown and simulation with similar parameters is shown on Fig.1. The experience that we gained using the PIC code to understand waveguide breakdown gives us confidence in applying the same method to study breakdown in accelerating structures.

ACCELERATING STRUCTURES

The characteristics of rf breakdown in traveling wave (TW) accelerating structures [5] are similar to those of waveguide breakdowns. The main similarities are: a drop off to zero of the transmitted rf power in tens of nanoseconds, with up to 80% of the incident rf energy absorbed after breakdown starts. We think that this analogy comes from some common characteristic of the waveguide and TW structures. Both have a broadband frequency response and are designed to transmit rf power. A breakdown that is localized in a limited volume or single cell does not change the ability of the structure to channel power to the breakdown site. We simulated 2D and 3D models of a TW accelerating structure. We used dimensions of a structure with an initial group velocity 0.05c that is currently under high power test at SLAC. We placed the emission spots on the iris of a structure cell. Results of PIC simulations of the accelerating structure lead to conclusions that are very similar to those for waveguides. We add some conclusions related to specifics of the accelerating structure below:

1. There is an asymmetry in the portion of electron current that exits through the beam apertures. Current is more likely to go toward the input coupler from the cell with the emission spot.
2. There is no significant difference between 2D and 3D models. Assuming the same total emission current, reflected power and transmitted rf power behave similarly in both models.
3. Electron current from the spot spreads over the inside surface of the cell, but the major part of the emitted current goes to a small area on an iris opposite to the emitting spot and to a current returning back to the emitting spot.
4. Secondary or back-scattered electrons do not change significantly the behavior of the rf fields.

Breakdown behavior of standing wave (SW) structures [1, 2] is very different from TW structures. In the TW case, a major part of the rf energy is absorbed by breakdown currents; in the SW case rf energy is reflected from the structure. After breakdown starts, reflected energy increases during ~100 ns in TW case, and in ~10 ns in SW case. We simulated a 2D SW structure to find the source of these differences. We used dimensions of the π phase advance SW structure that is currently under high power test at SLAC [5]. The simulated reflected power and a signal from a field probe are shown in Fig. 2. The main results of these simulations are listed below:

1. Electromagnetic fields in the structure collapse just after emission starts. Currents pass across the whole cavity and absorb a major part of the stored rf energy in a few nanoseconds, compared to a filling time of ~100 ns.
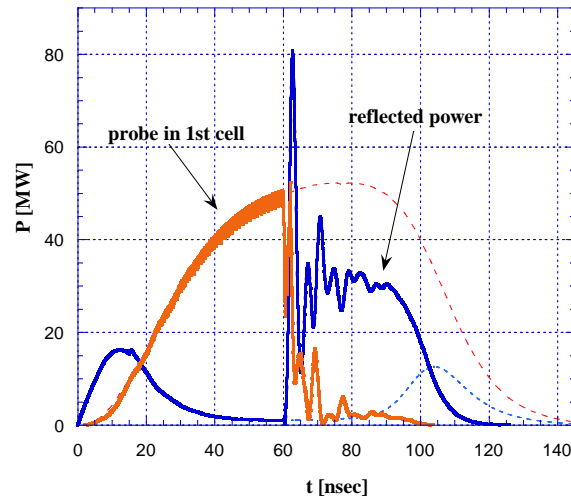
FIGURE 2. Reflected power and power from a simulated probe in the structure *vs.* time. Power from the probe is arbitrarily normalized. Emission starts at 60 ns. Dashed curves — no emission, solid curves — with emission.

2. The currents detune the whole structure, causing the π-resonance to shift from the working frequency. This shift causes rf energy to reflect from input iris of the structure.
3. The increase of the electric field in the cells (due to emitted currents) is generally smaller than for the TW structure.

The main difference between the TW and SW case is in the coupling of the structure cavity to the input waveguide. The goal in TW coupler design is to have a small reflection from the coupler over a wide frequency range ($\frac{\triangle f}{f} \sim 10^{-3}$). In the SW case, the goal is a small reflection from the beam-loaded structure in a narrow frequency range ($\frac{\triangle f}{f} \sim 10^{-4}$). In the TW case breakdown currents on the order of 10 A have a negligible effect on transmission and reflection of rf power, but in the SW case the same current shifts the resonant frequency enough to cause reflection of a major part of the incident rf power. We think that this high sensitivity of the SW structure to the breakdown currents may explain why the SW structures have reached higher maximum gradients than TW structures.

REFERENCES

1. G.A. Loew and J.W. Wang, SLAC-PUB-4647 (1988).
2. G.A. Loew and J.W. Wang, XIVth Int. Symp. on Disch. and Elec. Ins. in Vacuum, Santa Fe, New Mexico, September 16-20, 1990.
3. J.W. Wang *at al*, "High Gradient Tests of SLAC Linear Collider Accelerating Structures," SLAC-PUB-6617 (1994).
4. C. Adolphsen *at al*, "RF Processing of X-Band Accelerator Structures at the NLCTA," LINAC2000, August, 2000, Monterey, Ca.
5. C. Adolphsen *at al*, Paper ROAA003, PAC2001, June 18-22, 2001, Chicago, Illinois.
6. http://www.mrcwdc.com/Magic/